The Lipocalin LPR-1 Cooperates with LIN-3/EGF Signaling To Maintain Narrow Tube Integrity in *Caenorhabditis elegans*

Pu Pu, Craig E. Stone, Joshua T. Burdick, John I. Murray, and Meera V. Sundaram[1]
Department of Genetics, Perelman School of Medicine, University of Pennsylvania, Philadelphia, Pennsylvania 19104
ORCID ID: 0000-0002-2940-8750 (M.V.S.)

ABSTRACT Lipocalins are secreted cup-shaped glycoproteins that bind sterols, fatty acids, and other lipophilic molecules. Lipocalins have been implicated in a wide array of processes related to lipophilic cargo transport, sequestration, and signaling, and several are used as biomarkers for human disease, but the functions of most lipocalins remain poorly understood. Here we show that the *Caenorhabditis elegans* lipocalin LPR-1 is required to maintain apical membrane integrity and a continuous lumen in two narrow unicellular tubes, the excretory duct and pore, during a period of rapid lumen elongation. LPR-1 fusion protein is expressed by the duct and pore and accumulates both intracellularly and in apical extracellular compartments, but it can also function cell nonautonomously when provided from outside of the excretory system. *lpr-1* mutant defects can be rescued by increased signaling through the epidermal growth factor (EGF)-Ras-extracellular signal regulated kinase (ERK) pathway, which promotes the more elongated duct *vs.* less elongated pore tube fate. Spatial and temporal rescue experiments indicate that Ras signaling acts within the duct and pore tubes during or prior to cell fate determination to bypass the requirement for LPR-1. *lpr-1* mutations did not disrupt LIN-3/EGF-dependent duct-fate specification, prevent functioning of any specific LIN-3/EGF isoform, or alter LET-23/EGFR localization, and reduced signaling did not phenocopy or enhance *lpr-1* mutant defects. These data suggest that LPR-1 protects lumen integrity through a LIN-3/EGF-independent mechanism, but that increased signaling upregulates some target(s) that can compensate for *lpr-1* absence.

KEYWORDS *Caenorhabditis elegans*; excretory system; lipocalin; tubulogenesis; signaling

LIPOCALINS ("fat cups") are a large and diverse group of secreted glycoproteins that bind sterols, fatty acids, and other lipophilic molecules within the body. Members of the lipocalin family have limited sequence homology, but share a common secondary structure called the "lipocalin fold," which comprises an eight-stranded antiparallel β-barrel flanked by N- and C- terminal helices (Flower 1996). In mammals, lipocalins have been implicated in a wide array of processes related to lipophilic cargo transport, sequestration, and signaling. For example, retinol binding protein delivers dietary retinol (vitamin A) to target tissues with high retinol demand such as the eye (Quadro *et al.* 1999; Chou *et al.* 2015). Tear lipocalin transports and/or sequesters phospholipids within the tear film to enable proper lubrication of the eye (Glasgow *et al.* 1995; Gouveia and Tiffany 2005). Lipocalin2 (Lcn2, also known as 24p3 or neutrophil gelatinase associated lipocalin) sequesters iron-containing siderophores to protect against bacterial infections (Flo *et al.* 2004), and can influence signaling by hepatocyte growth factor during kidney tube development (Wu and Han 1994; Gwira *et al.* 2005; El Karoui *et al.* 2016). The lipocalin Swim (secreted interacting Wnt molecule) facilitates transport of lipid-modified Wnt ligands (Mulligan *et al.* 2012), and the plasma lipocalin apolipoprotein M (ApoM) facilitates transport of the signaling lipid sphingosine-1-phosphate (S1P) (Christoffersen *et al.* 2011). Humans have several dozen lipocalins, some of which are used as biomarkers for stress and diseases (*e.g.*, kidney disease, cardiovascular disease, airway disease, and dry eye disease) (Enriquez-de-Salamanca *et al.* 2012; Dittrich *et al.* 2013; Joshi and Viljoen 2015; Kashani and Kellum 2015), but the functions of most remain poorly understood.

doi: 10.1534/genetics.116.195156
Manuscript received August 23, 2016; accepted for publication December 21, 2016; published Early Online December 29, 2016.
Supplemental material is available online at www.genetics.org/lookup/suppl/doi:10.1534/genetics.116.195156/-/DC1.
[1]Corresponding author: 446A Clinical Research Bldg., 415 Curie Blvd., Philadelphia, PA 19104-6145. E-mail: sundaram@mail.med.upenn.edu

We showed previously that a mutation in the *Caenorhabditis elegans* lipocalin-related gene *lpr-1* disrupts integrity of the excretory duct and pore tubes within the excretory (renal-like) system (Stone *et al.* 2009). The excretory duct and pore are narrow unicellular tubes with an intracellular lumen (Figure 1, A–C). These tubes connect the larger excretory canal cell (also a unicellular tube) to the outside environment for fluid excretion. In *lpr-1* mutants, the tube cells are still connected in tandem via ring-shaped apical junctions, but the lumen is discontinuous, leading to a lethal defect in fluid excretion. *lpr-1* defects could be rescued by ectopic expression of *lpr-1* outside of the excretory system (Stone *et al.* 2009), suggesting that LPR-1 is involved in an extracellular transport or signaling mechanism important for lumen formation or maintenance.

Proper development of the *C. elegans* excretory system also requires epidermal growth factor (EGF) signaling through Ras and extracellular signal regulated kinase (ERK). During ventral enclosure, the duct and the pore cell precursors, which are initially equivalent and express the EGF receptor (EGFR) LET-23, migrate toward the canal cell, which expresses the EGF-like ligand LIN-3 (Abdus-Saboor *et al.* 2011). EGF-Ras-ERK signaling plays a critical role during duct *vs.* pore cell fate determination. Wild-type (WT) animals always have one duct and one pore, but increased signaling results in two duct cells and decreased signaling results in two pore cells (Abdus-Saboor *et al.* 2011). Following cell fate determination, the duct and pore form unicellular tubes by wrapping and forming auto-cellular junctions (AJs); the duct then rapidly auto-fuses to become a seamless toroid (Stone *et al.* 2009). By the 1.5-fold stage of embryogenesis, the canal cell, the duct cell, and the pore cell have connected to each other and formed a continuous lumen. Over the next several hours, the pore cell grows modestly, while the duct cell elongates dramatically. By the time the embryo hatches to a first stage (L1) larva, the duct has an asymmetric shape with a long, narrow process that links it to the pore cell, and a lumen that takes a winding path through the cell body (Figure 1, C and C′). In addition to promoting duct *vs.* pore cell fate determination, EGF-Ras-ERK signaling might be required for subsequent duct tube morphogenesis (Abdus-Saboor *et al.* 2011). Whereas null mutants lack an excretory duct, many hypomorphic EGF-Ras-ERK-pathway mutants have an abnormal duct cell with a cystic lumen. Requirements for EGF signaling in tube elongation have also been described in other model systems (Zhang *et al.* 2010; Saxena *et al.* 2014).

Given the similarities in the *lpr-1* and EGF-Ras-ERK-mutant phenotypes, we investigated the relationship between these pathways.

Materials and Methods

Strains and plasmids

Strains were grown according to the standard methods (Brenner 1974) and maintained at 20° unless otherwise noted. Bristol N2 was the WT strain. See Supplemental Material, File S1 for a complete list of strains used in this study. See File S2 for details about plasmid construction. *lpr-1(cs207)* (Q72stop) and *lpr-1(cs209)* (W217stop) were isolated as rod-like lethal mutants after standard EMS mutagenesis (Brenner 1974) of strain UP2214 (see File S1). Alleles were outcrossed twice before analysis. *sos-1(pd10gf)*, an E99K missense substitution, was isolated by N. Hopper (personal communication) in a screen for suppressors of *sem-5(n1619lf)* lethality. *pd10* is inferred to be a gain-of-function (gf) allele based on this suppressor property, although it causes no apparent single mutant phenotype.

Construction of extrachromosomal transgenic strains

Transgenic animals were generated by injecting N2 with plasmid DNA at 10–20 ng/μl together with transgenic markers pCFJ90 (*myo-2p*::mCherry) (3 ng/μl) or pRF4 [*rol-6*(*su1006*)] (80 ng/μl) or pIM175 (*unc-119p*::GFP) (100 ng/μl) and pSK+ to a total DNA concentration of 150–200 ng/μl.

Construction of lin-3 mos1-mediated single copy insertion transgenic strains

lin-3 complementary DNAs (cDNAs) were a generous gift from Cheryl Van Buskirk (California State University, Northridge, CA) and Paul Sternberg (California Institute of Technology, Pasadena, CA). Complete sequences of these cDNAs are given in File S3. *lin-3* cDNAs were inserted within mos1-mediated single copy insertion (MosSCI) destination clone pCFJ150 or pCFJ151 (Frokjaer-Jensen *et al.* 2008), downstream of a proximal 1987 bp *lin-3* promoter containing the first *lin-3* intron and an artificial stop codon. See Extended Materials and Methods File S2 for details.

Single copy transgene lines were obtained by microinjection of the expression constructs (pEP36, pEP46, pEP47) at 10 ng/μl with co-injection markers pCFJ90 (*myo-2p*::mCherry) at 3 ng/μl, pCFJ104 (*myo-3p*::mCherry) at 5 ng/μl, pGH8 (*rab-3p*::mCherry) at 10 ng/μl, and transposase plasmid pCFJ601 (*elt-3p*::mosase) at 50 ng/μl into strain EG4322. Insertions into chromosome *II* were verified by PCR using primers flanking the insertion (Frokjaer-Jensen *et al.* 2008). None of the integrated *lin-3* transgenes caused a Multivulva phenotype, consistent with modest levels of expression.

Embryonic RNA sequencing analysis

Temporal RNA sequencing (RNA-seq) data were downloaded from modENCODE (http://www.modencode.org; Gerstein *et al.* 2010). Lineage-specific RNA-seq data were obtained from our prior study (Burdick *et al.* 2016); these reads are available in the Sequence Read Archive (SRA) at accession SRX1272936 (*pros-1*), SRX1272933 (*unc-130*), SRX1272898 (*ceh-6*), and SRX1272935 (*ceh-6*+*hlh-16*). Reads were aligned to the WS220 genome using Tophat 2 (Trapnell *et al.* 2009). For the modENCODE data, we quantified isoforms using Cufflinks, with default settings (Trapnell

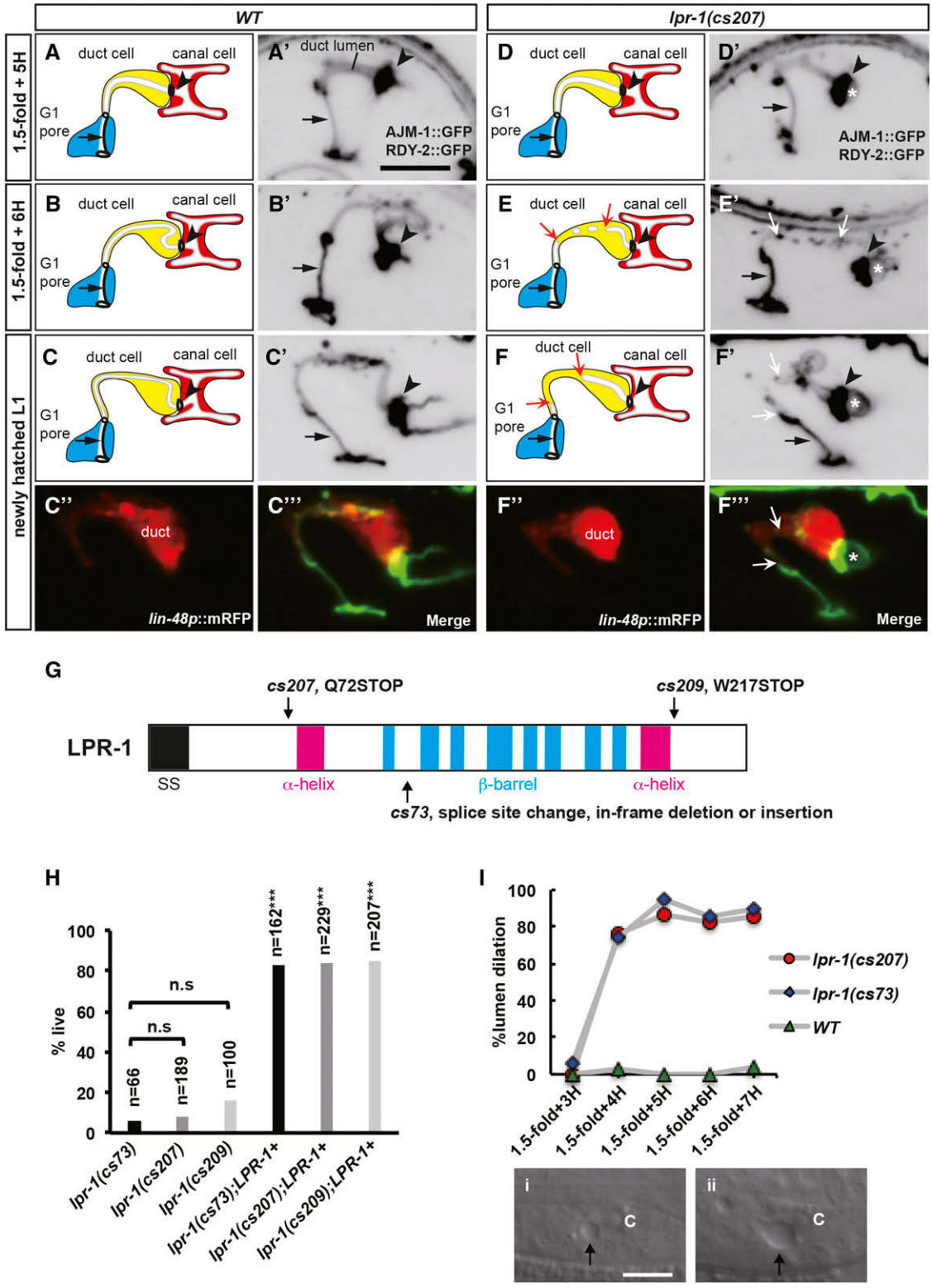

Figure 1 *lpr-1* null mutants have incompletely penetrant defects in duct and pore lumen maintenance. (A–F) Schematic representations of excretory system morphology in (A–C) WT and in (D–F) *lpr-1(cs207)*. G_1 pore cell is shown in blue, duct cell in yellow, canal cell in red. White regions represent lumen. Heavy black lines represent apical junctions. Arrowhead, duct-canal intercellular junction. Anterior is to the left and ventral is down in all images. (A′–F′) Progressive lumen fragmentation in *lpr-1* mutants. Inverted grayscale fluorescent images of (A′–C′) WT and (D′–F′) *lpr-1(cs207)* animals expressing the apical membrane marker RDY-2::GFP and junction marker AJM-1::GFP. * marks lumen dilation near the canal-duct junction. White arrows point to the breakage of the duct lumen. Black arrows indicate pore AJ. (C″ and F″) Show the duct cell marker *lin-48p*::mRFP (red), which is overlaid with the lumen and junction markers in (C‴ and F‴) to show that the duct cell and pore cell were still connected to each other. Bar, 5 μm. (G) Schematic representation of

et al. 2010). For the lineage-specific data, we manually counted reads visualized using the Integrative Genomics Viewer (Robinson *et al.* 2011).

Microscopy and imaging

Differential interference contrast (DIC) and epifluorescence microscopy were performed using a Carl Zeiss (Thornwood, NY) Axioskop, and images were taken with a Q1CAM monochrome charge-coupled device camera. All confocal microscopy was performed on a Leica TCS SP8 multiphoton microscope. Images were processed for brightness and contrast by ImageJ or Fiji (Schindelin *et al.* 2012; Schneider *et al.* 2012).

Scoring of viability

For most experiments, young adult hermaphrodites were allowed to lay eggs for a few hours. Then, adults were removed and the number of embryos was counted. Two days after egg laying, the number of live worms was counted. The live percentage = live worms/eggs laid. For transgenic rescue experiments, the genotype of unhatched eggs could not be assessed reliably, so these were excluded and the live percentage = live worms/live worms + rods. Since the number of unhatched eggs was generally low (<5%), ignoring them would not have a major impact on the outcome.

Scoring of lumen dilation

Lumen dilation was visualized by DIC as a small bubble adjacent to the canal cell nucleus. Then, 1.5-fold-stage eggs were picked onto seeded NGM plates and incubated at 20° for the indicated number of hours prior to microscopy, or threefold-stage eggs were picked onto seeded NGM plates and 40 min later newly hatched L1 larvae were mounted for microscopy.

Heat-shock experiments

Young adult hermaphrodites were allowed to lay eggs at 20° for 1 hr. Adults were removed and the number of embryos on each plate was counted. Eggs were incubated at 20° for the indicated number of hours prior to heat shock at 31° for 1 hr. The number of embryos that had survived to L3 larvae was counted 2 days later.

Scoring of duct and pore cell fates

Duct and pore cell fates were assessed in late threefold embryos or early L1 larvae based on the pattern of the junction marker AJM-1::GFP (Koppen *et al.* 2001), as visualized by epifluorescence microscopy. The duct is a seamless tube and lacks AJM-1::GFP signal along its length, whereas the pore has an AJ (Abdus-Saboor *et al.* 2011). We also confirmed cell fates in *WT*, *lpr-1(cs207)*, *LIN-3 overexpression* (*OE*), and *lpr-1(cs207)*; *LIN-3 OE* by examining the duct cell markers *lin-48p*::mRFP (Parry and Sundaram 2014) and *lin-48p*::NLS::GFP.

Vulva induction assay

Vulva induction was scored by counting induced and uninduced vulval precursor cells by DIC at the L4 stage as described (Sternberg and Horvitz 1986; Han *et al.* 1990).

Data availability

Strains and plasmids are available upon request. File S1 contains detailed descriptions of all strains. File S2 contains information about all plasmids. File S3 contains specific *lin-3* cDNA sequences used. RNA-seq data are available in the SRA at accession SRX1272936 (*pros-1*), SRX1272933 (*unc-130*), SRX1272898 (*ceh-6*), and SRX1272935 (*ceh-6*+*hlh-16*).

Results

lpr-1 null mutants have an incompletely penetrant defect in duct lumen maintenance during tube elongation

The original allele of *lpr-1*, *cs73*, is a splice donor mutation that strongly reduces but may or may not eliminate gene function (Stone *et al.* 2009). In a genetic screen for additional *lpr-1*-like mutants (see *Materials and Methods*), we identified two new nonsense alleles that are predicted to truncate the LPR-1 protein just prior to or just after the β-barrel domain (Figure 1G); the former, *lpr-1(cs207)*, should be a molecular null allele. Both new alleles caused incompletely penetrant cystic duct and lethal phenotypes similar to those of *lpr-1(cs73)* mutants, and both were efficiently rescued by a WT *lpr-1* transgene (Figure 1, H and I). Mutant animals that escaped lethality were fertile and laid eggs normally. We conclude that the *lpr-1* null phenotype is incompletely penetrant.

Prior studies did not distinguish between requirements for *lpr-1* in initial lumen formation or maintenance. To address this issue, we compared *WT* and *lpr-1* mutants over a time course of development (Figure 1, A′–F′). *lpr-1* mutants had one pore and one duct as in WT (Figure S1), and initial steps of duct and pore tube development appeared normal based on the expression patterns of the apical junction marker AJM-1::GFP and the apical membrane marker RDY-2::GFP (Figure 1D). Duct lumen discontinuities and cysts first appeared during tube elongation in the latter part of embryogenesis (Figure 1, E′ and I). In most newly hatched L1 larvae, duct

LPR-1 protein and the positions of three mutant alleles. Allele *cs207* is a C to T transition at the first nucleotide of codon 72, which results in a premature stop. Allele *cs209* is a G to A transition at the third nucleotide of codon 217, which results in a premature stop. Allele *cs73* affects a splice donor site, as described previously (Stone *et al.* 2009). SS, secretion signal peptide. (H) All three mutant alleles of *lpr-1* were rescued by multi-copy transgenes containing *lpr-1* genomic DNA. ***$P < 0.0001$ compared to *lpr-1* mutants (Fisher's exact test). n.s, not significant. (I) Time line of lumen dilation in *lpr-1* mutants. Lumen dilation was visualized by DIC as a small bubble anterior to the canal cell nucleus. (i) At 1.5-fold plus 4 hr stage, the size of the lumen bubble was similar to the size of the canal nucleolus and adjacent to it. (ii) At later stages, the bubble size increased. Scale bar, 5 microns.

cell shape appeared normal and the duct and pore cells were still connected by an apical junction, despite absence of lumen in the distal region of the duct (Figure 1F′). We conclude that *lpr-1* is not required for *de novo* lumen formation but is important to maintain duct and pore lumen integrity during elongation.

In addition to *lpr-1*, the *C. elegans* genome contains at least six other lipocalin-related (*lpr*) genes, four of which share sequence homology with *lpr-1* (Figure S2). Transgenic cross-rescue experiments using three of the most closely related other *lpr* genes (*lpr-3*, *lpr-4*, and *lpr-5*) did not support the hypothesis that incomplete penetrance of *lpr-1* mutants is explained by redundancy with another lipocalin (Figure S2).

LPR-1 localizes to both intracellular and apical extracellular compartments

An *lpr-1* transcriptional reporter is expressed in most external (cuticle-producing) epithelia, including both the duct and pore cells and the epidermis, but not in internal epithelia such as the gut or excretory canal cell (Stone *et al.* 2009). Importantly, however, LPR-1 contains a predicted signal peptide and can function cell nonautonomously when ectopically expressed, suggesting that it is a secreted protein that can be provided from outside of the excretory system (Stone *et al.* 2009).

To determine the localization of the LPR-1 protein, we analyzed fusions tagged either N-terminally or C-terminally with GFP or with Superfolder GFP, a variant that folds more rapidly and fluoresces more brightly than standard GFP when present in oxidizing extracellular environments (Aronson *et al.* 2011). When driven by the *lpr-1* promoter, all fusions rescued *lpr-1* lethality (Figure 2A) and were detected within the duct and pore cells and other external epithelia beginning at the 1.5-fold stage (Figure 2, B and C). The fusions were also secreted apically between the embryo and the eggshell (Figure 2, B, D, and E) and appeared enriched in or near the duct and pore lumens at the threefold stage (Figure 2, D and F). N-terminally GFP-tagged LPR-1 lacking a signal sequence was not detectably secreted at all (Figure 2G) and failed to rescue *lpr-1* lethality (Figure 2A), indicating that secretion is indeed important.

We also compared LPR-1 fusion localization when driven by other promoters. When driven by the *grl-2* promoter, ssGFP::LPR-1 accumulated specifically within the duct and pore cells, and was not detected extracellularly (Figure 2H); suggesting that the duct/pore luminal signal detected previously may reflect protein that originated elsewhere and entered the lumen from the extraembryonic space. When driven by the *unc-54* body muscle promoter, ssGFP::LPR-1 accumulated within muscle cells (Figure 2I) and also was secreted into the pseudocoelom and accumulated in coelomocytes, scavenger-like cells that take up most internally secreted proteins (Fares and Greenwald 2001) (Figure 2J), but it did not accumulate detectably near or within the duct and pore (Video 1 in File S4). Nevertheless, both duct-pore-expressed and muscle-expressed ssGFP::LPR-1 were equally effective at rescuing *lpr-1* lethality (Figure 2A). We conclude that LPR-1 (or some downstream effector) can travel between cells and that its specific site of synthesis is relatively unimportant. LPR-1 may exert its functions extracellularly and/or within an endocytic compartment. If LPR-1 acts directly on the duct and pore, very low levels (undetectable by fluorescence) must be sufficient to rescue *lpr-1* excretory tube defects.

Hyperactivation of EGF-Ras-ERK signaling during duct and pore tubulogenesis rescues lpr-1 lethality

Nonautonomous action of LPR-1 is consistent with involvement in some signaling or transport mechanism. We showed previously that EGF-Ras-ERK signaling promotes excretory duct identity (Abdus-Saboor *et al.* 2011) (Figure 3A), and the excretory duct elongates much more than the excretory pore (Figure 1C). Therefore, EGF-Ras-ERK signaling promotes tube elongation, either directly or indirectly, making this a pathway of interest.

To test the relationship between *lpr-1* and EGF-Ras-ERK signaling, we analyzed double mutants. *lpr-1* mutant lethality was significantly suppressed by OE from a *lin-3*/EGF genomic construct, by hyperactivating mutations in LET-60/Ras or its guanine nucleotide exchange factor SOS-1, or by loss of the MPK-1/ERK target LIN-1/Ets (Figure 3B and Figure S3). Additionally, *lpr-1* lethality was slightly rescued by *lin-15(n765)* (Figure 3B), a mutant with low levels of ectopic LIN-3/EGF expression due to modest derepression of *lin-3* transcription (Cui *et al.* 2006; Saffer *et al.* 2011). Conversely, LPR-1 OE could not suppress lethality of a hypomorphic *let-60 ras* mutant (Figure S3). These epistasis data suggest that *lpr-1* functions either upstream of or in parallel to *lin-3*/EGF to affect duct and pore lumen integrity.

Hyperactivation of EGF-Ras-ERK signaling often results in a pore-to-duct fate transformation (zero pore, two duct phenotype), and the two duct cells then fuse to make a binucleate duct tube (Abdus-Saboor *et al.* 2011) (Figure 3, A and C). *lpr-1(cs207)* did not affect such cell fate changes caused by *lin-15* loss, *lin-3* OE, or a *let-60/ras* gf mutation (Figure 3C and Figure S1). *lpr-1(cs73)* appeared to have a small effect on cell fates in the *lin-15* background, but this may be explained by genetic background effects, since the effect was unique to this allele (Figure S3). Reduced EGF-Ras-ERK signaling often results in the opposite duct-to-pore fate transformation (two pore, zero duct phenotype) (Abdus-Saboor *et al.* 2011) (Figure 3A). *lpr-1(cs207)* did not cause such cell fate changes, even in a sensitized *sos-1* hypomorphic background (Figure S1 and Figure S3). Therefore, *lpr-1* loss does not appear to broadly disrupt signaling.

Pore-to-duct cell fate changes did not correlate with the degree of *lpr-1* suppression. For example, *sos-1(pd10gf)*, a gf allele of the major Ras guanine nucleotide exchange factor (Chang *et al.* 2000) (N. Hopper, personal communication; see *Materials and Methods*), did not cause cell fate transformations (Figure 3C) but strongly suppressed *lpr-1* lethality

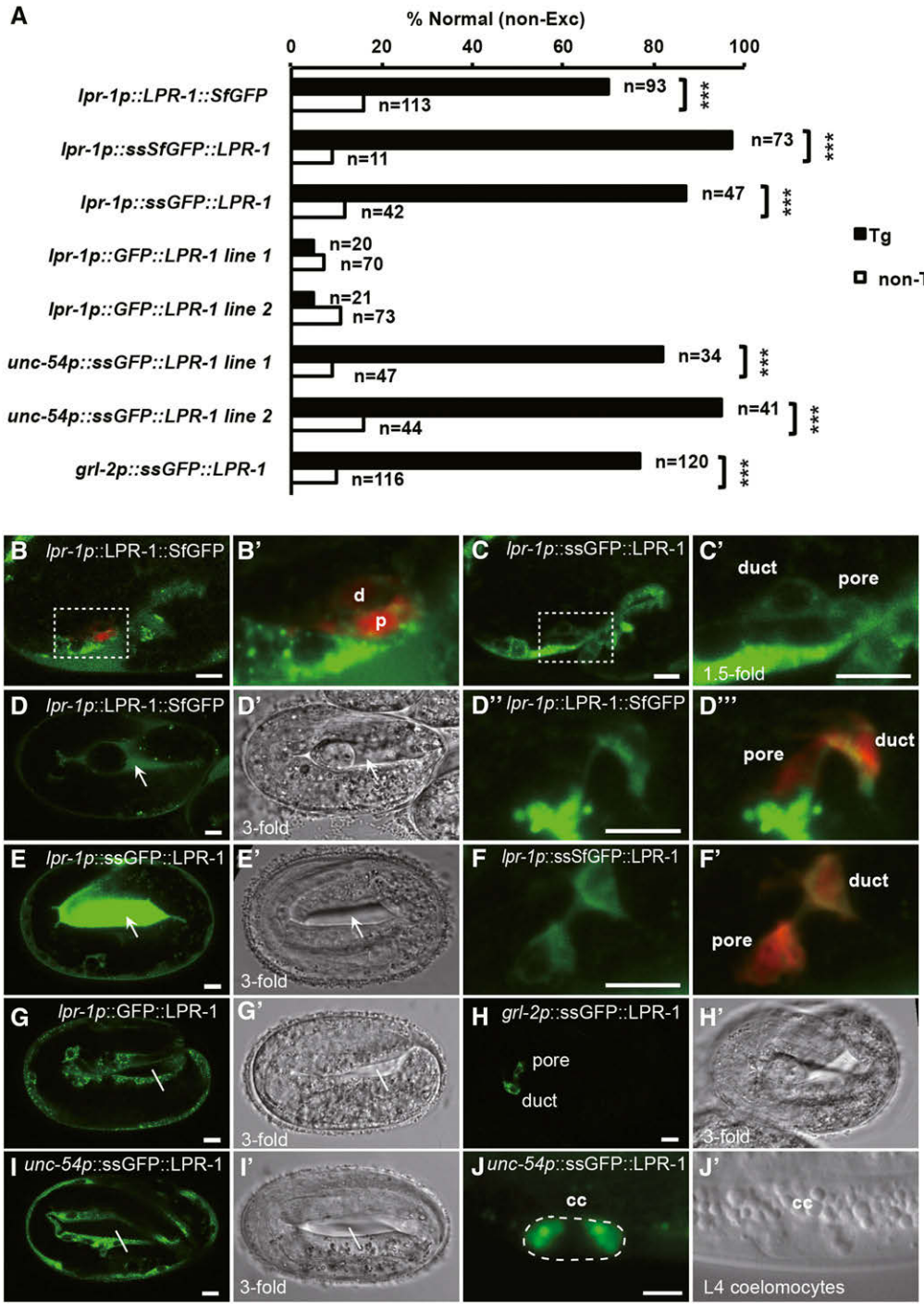

Figure 2 LPR-1 functions cell nonautonomously and localizes both extracellularly and intracellularly. (A) Rescue ability of various transgenes expressing GFP-tagged LPR-1 with or without a signal sequence. Bars indicate percentage of transgenic (Tg) (black) or non-transgenic (non-Tg) (white) animals showing normal excretory tube morphology at the L1 stage as assessed by DIC microscopy. ***$P < 0.0001$ compared to non-transgenic siblings (Fisher's exact test). (B and B′) Expression pattern of *lpr-1p*::LPR-1::SfGFP at 1.5-fold. Duct and pore cells are marked by *grl-2p*::mRFP (red). (C and C′) Expression pattern of *lpr-1p*::ssGFP::LPR-1(25-261) at 1.5-fold. Boxes in (B) and (C) indicate the regions magnified in (B′) and (C′). (D, D′, D″, and D‴) Expression pattern of *lpr-1p*::LPR-1::SfGFP at threefold. (D″) and (D‴) show a confocal projection of the duct and pore from the same embryo. White arrows indicate fusion protein accumulating in the space between the embryo and the eggshell. (E and E′) Duct and pore cells are marked by *grl-2p*::mRFP. (F and F′) *lpr-1p*::ssGFP::LPR-1(25-261) was expressed in the epidermis and accumulated in the space between the embryo and the eggshell, indicated by white arrows. In an early threefold embryo, *lpr-1p*::ssSfGFP::LPR-1(25-261) was enriched cortically in the duct and pore (marked in red). (G and G′) *lpr-1p*::GFP::LPR-1(25-261) lacking a signal peptide was restricted in epithelia and not secreted. White lines indicate the space between the embryo and the eggshell. (H and H′) *grl-2p*::ssGFP::LPR-1(25-261) was only detectably expressed in the duct and pore cells ($n = 37$). (I and I′) *unc-54p*::ssGFP::LPR-1(25-261) was not secreted apically from embryos, but (J and J′) accumulated in coelomocytes (cc) in larvae. Bar, 5 μM.

(Figure 3B and Figure S3). Conversely, *lin-15(n765)* caused cell fate transformations at moderate frequency (Figure 3C), but was a relatively weak suppressor of *lpr-1* lethality (Figure 3B and Figure S3). We therefore conclude that upregulation of EGF-Ras-ERK signaling bypasses the need for LPR-1 through a mechanism that is independent of changes in pore cell identity and the associated changes in AJs and intercellular junctions.

To test if Ras signaling in the excretory duct and pore is sufficient to rescue *lpr-1* mutants, we expressed constitutively active LET-60/Ras(G13E) under control of the *grl-2* promoter, which drives expression in the duct, pore, and a small number of other cells in the nose and tail (Hao *et al.* 2006) (Figure 2F). *grl-2p*::LET-60(G13E) caused pore-to-duct cell fate transformation and significantly rescued *lpr-1* lethality (Figure 3D and Table 1). In contrast, transgenes expressing

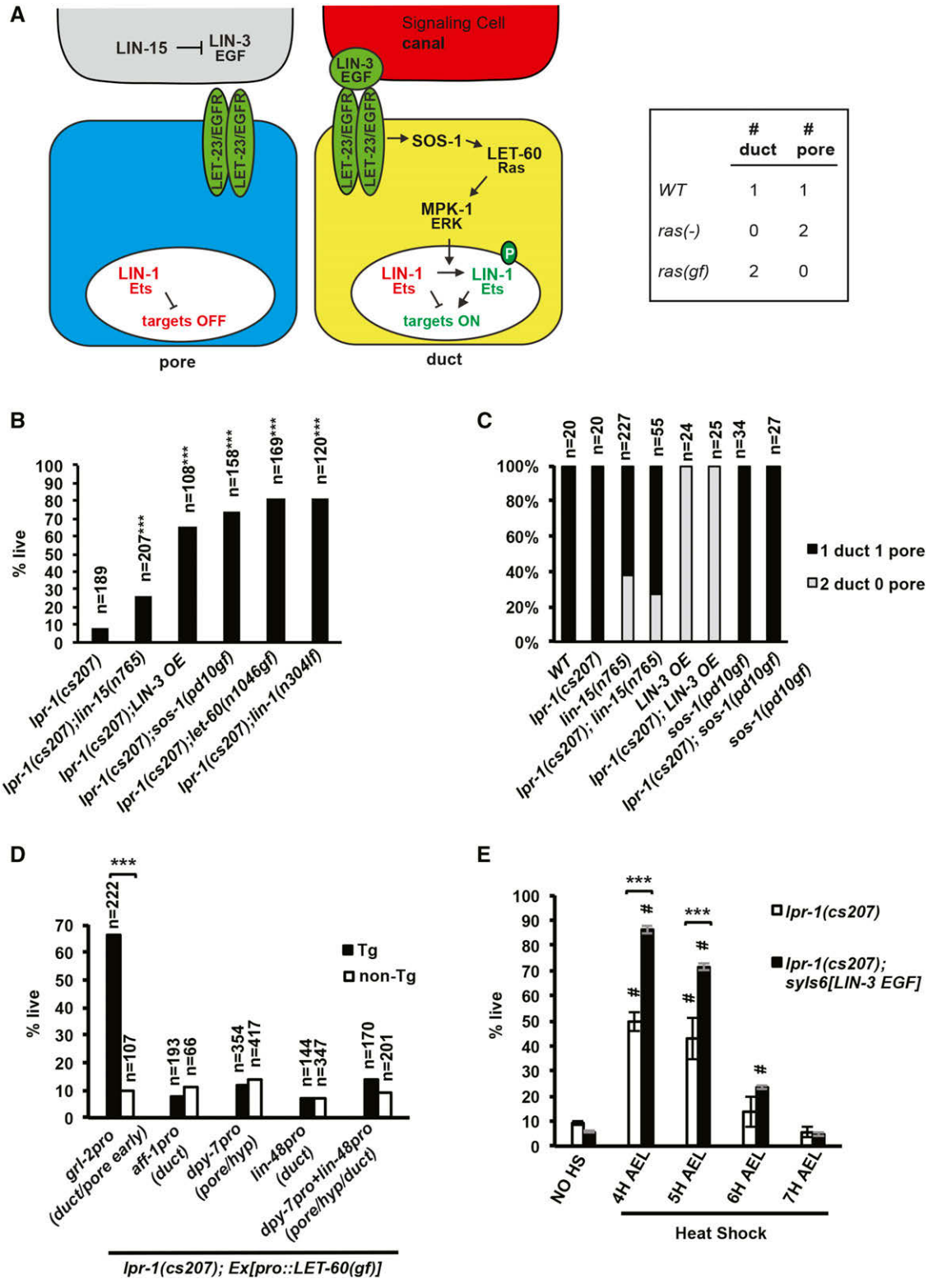

Figure 3 Constitutive EGF-Ras-ERK signaling in the duct and pore bypasses the requirement for *lpr-1*. (A) Schematic representation of the major components of the EGF-Ras-ERK signaling pathway in the excretory system. Duct in yellow, pore in blue, canal in red. (B) Epistasis analysis between *lpr-1(cs207)* and components of EGF-Ras-ERK-signaling pathway. Viability of animals of the indicated genotypes is shown. LIN-3 OE was achieved with an integrated *lin-3p*::LIN-3::GFP transgene provided by Min Han. ***$P < 0.001$ compared to *lpr-1(cs207)* (Fisher's exact test). (C) Loss of LPR-1 did not affect duct *vs.* pore cell fate determination. Quantification of cell fate in threefold embryos, duct *vs.* pore cell fates were assessed by AJM-1::GFP marker. (D) Effects of tissue-specific expression of LET-60/Ras(G13E) on the viability of *lpr-1(cs207)*. The *grl-2* promoter is active prior to duct and pore cell fate determination ("early") based on the ability of *grl-2p*::LET-60(G13E) to cause a cell fate switch (see Table 1). The *aff-1* and *dpy-7* promoters are active by

LET-60(G13E) slightly later in the duct (*aff-1* or *lin-48* promoters) or in the pore and hypodermis (*dpy-7* promoter) did not rescue, even when combined (Figure 3D). These data suggested that increased signaling may be required in one or both cells prior to duct and pore cell fate determination.

As another approach to determine when signaling is relevant, we used an inducible heat-shock promoter to express the LIN-3 EGF domain at different stages of embryonic development (Figure 3E). Surprisingly, we found that heat shock alone partly rescued *lpr-1(cs207)* lethality (Figure 3E). This result might be explained by a recent report that heat stress upregulates LIN-3/EGF signaling activity (Hill *et al.* 2014), although heat shock alone did not induce pore-to-duct cell fate transformations expected for strong LIN-3/EGF upregulation (Table 1). Heat-shock-induced OE of the LIN-3 EGF domain did induce pore-to-duct cell fate transformations (Table 1) and rescued *lpr-1(cs207)* lethality more completely than heat shock alone, with the best rescue obtained when heat shock was applied at the bean stage (Figure 3E). Heat shocks after the twofold stage had no beneficial effect (Figure 3E). Analogous rescue results were also obtained in *lpr-1(cs209)* and *lpr-1(cs73)* mutant backgrounds (data not shown). These results prove that OE of the active form of LIN-3/EGF is sufficient to rescue the *lpr-1(lf)* excretory defect. Considering the 0.5–1 hr delay from heat shock to functional protein production (Bacaj and Shaham 2007), these time course results suggest that increased LIN-3/EGF signaling during cell fate specification and early steps of duct and pore tubulogenesis (comma stage and 1.5-fold stage) is required to rescue the *lpr-1* lumen integrity defect.

The predominant LIN-3/EGF isoform in the canal cell has relatively weak signaling activity

The epistasis data above could be consistent with a model where LPR-1 facilitates LIN-3/EGF signaling from the canal cell to the duct. However, such a model would have to explain why LPR-1 facilitates signaling for lumen elongation, yet does not seem to affect cell fate specification. Therefore, we considered the possibility that different LIN-3 isoforms are specialized for different functions. LIN-3 is the only EGF-related ligand in *C. elegans*, but alternative splicing generates at least four LIN-3 protein isoforms (S, L, XL, and XXL) that differ in their extracellular juxtamembrane domains (Figure 4, A and B) (Dutt *et al.* 2004; Van Buskirk and Sternberg 2007; Gerstein *et al.* 2010). These isoforms may differ in binding partners or in susceptibility to proteolytic cleavage (Dutt *et al.* 2004), which typically releases the active EGF domain from the transmembrane precursor (Rose-John 2013; Adrain and Freeman 2014). Prior OE studies have revealed some functional differences among these LIN-3 isoforms (Dutt *et al.* 2004; Van Buskirk and Sternberg 2007), but their individual expression patterns and requirements are not known.

To determine which *lin-3* splice isoforms are expressed during embryonic development, we analyzed publicly available temporal RNA-seq data from the modENCODE project (Gerstein *et al.* 2010). The two shortest *lin-3* isoforms, S and L, were present in very early embryonic stages, when most messenger RNAs (mRNAs) are maternally derived, but then declined precipitously by the 200 min time point. After the birth of the excretory canal cell at ~300 min, the S, L, and XL *lin-3* isoforms were detected; with the S isoform at consistently modest levels, the L isoform at lower levels, and the XL isoform becoming progressively more predominant at later time points (Figure 4E).

To determine which *lin-3* splice isoforms are expressed in the excretory canal cell, we analyzed RNA-seq data from FACS-sorted embryonic cell populations that include the canal cell (Burdick *et al.* 2016). We examined RNA-seq reads from four cell populations, sorted on the basis of the canal cell lineage markers *ceh-6*, *pros-1*, and *unc-130*, as well as a more specific population of cells expressing *ceh-6* but not *hlh-16*. Of reads crossing the relevant *lin-3* exon boundaries (Figure 4A), 44 supported inclusion of the cassette exon unique to LIN-3(XL) and LIN-3(XXL), while only 10 reads supported cassette exon skipping. Specifically, seven reads corresponded to *lin-3(S)*, three to *lin-3(L)*, eight to *lin-3(XL)*, and one to *lin-3(XXL)*, while 35 additional reads corresponded to either *lin-3(XL)* or *lin-3(XXL)*, but did not cover the 5′ splice junction to distinguish between these. Together with the modENCODE data above, these results suggest that multiple LIN-3 isoforms are expressed by the canal cell, but that LIN-3(XL) is likely the predominant isoform.

To test which of these LIN-3 isoforms can promote excretory duct development and rescue *lpr-1* mutants, we compared the ability of each isoform to rescue *lin-3* and *lpr-1* null mutant phenotypes. To facilitate such comparisons and to mimic the endogenous expression pattern as closely as possible, each *lin-3* isoform was expressed under the control of the proximal *lin-3* promoter, which is active in the canal cell and gonadal anchor cell (Figure 4, C and D), and transgenes were introduced into the genome at single copy using the MosSCI technique (Frokjaer-Jensen *et al.* 2008). All three isoforms could rescue *lin-3(n1059)* lethality (Figure 4F) and

the 1.5-fold stage (Gilleard *et al.* 1997; Stone *et al.* 2009). The *lin-48* promoter was reported to come on at 1.5-fold (Wang *et al.* 2006), but we typically detect its activity at the threefold stage. ***$P < 0.0001$ compared to nontransgenic siblings (Fisher's exact test). (E) Viability of *lpr-1(cs207)* or *lpr-1(cs207)* carrying the transgene *syIs6 [hsp16.41p::LIN-3 EGF]* after heat shock at 31° for 1 hr at the indicated number of hours (H) after egg lay (AEL). Stages correspond roughly to bean (4 H AEL), comma (5 H AEL), twofold (6 H AEL) and threefold (7 H AEL) (See *Materials and Methods* for details). At least 70 animals were counted per experiment, and three experiments performed for each genotype. Error bars indicate SE. *P*-value from two tailed *t*-test: ***$P < 0.001$, heat-shocked *lpr-1(cs207); syIs6* compared to heat-shocked *lpr-1(cs207)* control. #$P < 0.001$, heat-shocked *lpr-1(cs207)* or heat-shocked *lpr-1(cs207); syIs6* compared to their nonheat-shocked control. n.s, not significant.

Table 1 *lpr-1* suppression does not correlate with pore-to-duct cell fate transformation

Genotype	Viability (*N*) (%)	Animals with two ducts (*N*) (%)
lpr-1(cs207); jcIs1	6 (97)	0 (26)
lpr-1(cs207); jcIs1 HS[a]	53 (208)	0 (31)
lpr-1(cs207); syIs6 [hsp-16.41p::LIN-3(EGF)]^; jcIs1 HS[b]	67 (61)	53 (36)
lpr-1(cs207); csEx455 [grl-2p::LET-60(gf)]; jcIs1	65 (93)	100 (28)

Two parallel plates containing eggs of the indicated genotypes were used to determine viability and the percentage of animals having two duct cells, respectively. Animals on one plate were scored at the threefold stage for duct and pore cell fates using the junction marker *jcIs1 [AJM-1::GFP]*. Animals on the other plate were scored for viability 2 days later. HS, heat shock.

[a] Heat shock at bean stage at 31° for 1 hr, returned to 20°.

[b] *syIs6* generated by Katz *et al.* (1995).

duct fate (Figure 4G); but they differed markedly in their ability to rescue vulval development (Figure 4H), another LIN-3/EGF-dependent process (Hill and Sternberg 1992; Katz *et al.* 1995). The isoforms also differed in their ability to induce pore-to-duct cell fate transformations in a WT background (Figure 4I), and to rescue *lpr-1(cs207)* lethality (Figure 4J), with LIN-3XL having the weakest activity. Duct development involves signaling between cells that directly contact each other (Figure 3A), whereas pore-to-duct fate transformation and vulva development involve signaling between cells that are separated by intervening cells or by a basement membrane (Abdus-Saboor *et al.* 2011; Gupta *et al.* 2012). The weak activity of LIN-3(XL) in the two latter assays suggests this isoform does not signal efficiently at a distance.

In summary, these data show that multiple LIN-3 isoforms can function in excretory development, but that the predominant excretory canal isoform, LIN-3XL, has relatively weak signaling activity compared to LIN-3S or LIN-3L. Therefore, excretory system development may be particularly sensitive to the loss of factors that normally facilitate LIN-3 signaling or its downstream consequences. However, because each LIN-3 isoform could rescue duct fate and at least partially bypass the requirement for LPR-1, even when modestly overexpressed (Figure 4J), no isoform appears specialized for lumen elongation or completely reliant on LPR-1 for its signaling activity.

LET-23/EGFR localizes to apical membranes during tube elongation

We previously showed that a functional LET-23/EGFR::GFP reporter was expressed on the surfaces of the presumptive duct and pore prior to cell fate determination and tube formation (Abdus-Saboor *et al.* 2011). To examine the dynamic expression pattern of LET-23 in the excretory system, we took advantage of a newer functional LET-23::GFP reporter that is expressed at endogenous levels and more closely mimics the pattern observed by immunolocalization (Haag *et al.* 2014). From comma to twofold stage, when the duct and pore first form tubes, LET-23::GFP was moderately expressed at the basolateral surface of the duct and pore cells, and highly expressed at the apical surface of the developing tubules (Figure 5, A and B). For the remainder of embryogenesis, LET-23::GFP was detected only at the apical surface of the elongating tubules (Figure 5C). LET-23::GFP localization was not noticeably different in *lpr-1* mutants (Figure S4).

EGF signaling promotes duct tube elongation through a mechanism that is closely coupled to duct fate determination

The duct tube elongates much more dramatically than does the pore tube (Figure 1C), and the spatial and temporal expression pattern of LET-23::GFP is consistent with prior suggestions that continued EGF signaling could play a direct role in the duct elongation process (Abdus-Saboor *et al.* 2011). To test for such a role, we used the temperature-sensitive allele *sos-1(cs41ts)* (Rocheleau *et al.* 2002; Abdus-Saboor *et al.* 2011) and examined apical membrane morphology using RDY-2::GFP. When upshifted to restrictive temperature at the 1.5-fold stage (after cell fate determination), *sos-1(cs41ts)* embryos showed normal duct elongation and no evidence of lumen fragmentation or dilation until well after hatch ($n = 19$), when defects in G_1 pore delamination become apparent (Parry and Sundaram 2014). These defects in pore delamination likely explain the cystic lumens originally observed by Abdus-Saboor *et al.* (2011). When upshifted before cell fate determination, rare *sos-1(cs41ts)* animals with normal cell fates still had normal lumen morphology ($n = 2$; Figure S5), while those animals with two G_1 pore cells and no duct had a shorter lumen but no evidence of fragmentation or dilation prior to hatch ($n = 11$; Figure S5). These experiments did not provide any evidence that continued EGF signaling through SOS-1 is required for duct tube elongation or for general lumen integrity. Instead, signaling appears to promote duct tube elongation through a mechanism that is temporally coupled to duct fate determination.

As an alternative approach to test the role of EGF-Ras-ERK signaling, we asked if reducing signaling could enhance the incompletely penetrant lumen defects of *lpr-1* mutants. At 20°, *sos-1(cs41ts)* mutants appear normal but genetically interact with other signaling mutants, suggesting hypomorphic activity (Rocheleau *et al.* 2002). Double mutants between *lpr-1(cs207)* and *sos-1(cs41ts)* did not show enhanced lethality compared to *lpr-1* mutants alone (Figure S5). Similarly, double mutants between *lpr-1(cs207)* and the hypomorphic mutant *mpk-1(ku1)* (Wu and Han 1994) did not show enhanced lethality (Figure S5). Therefore, despite the fact that

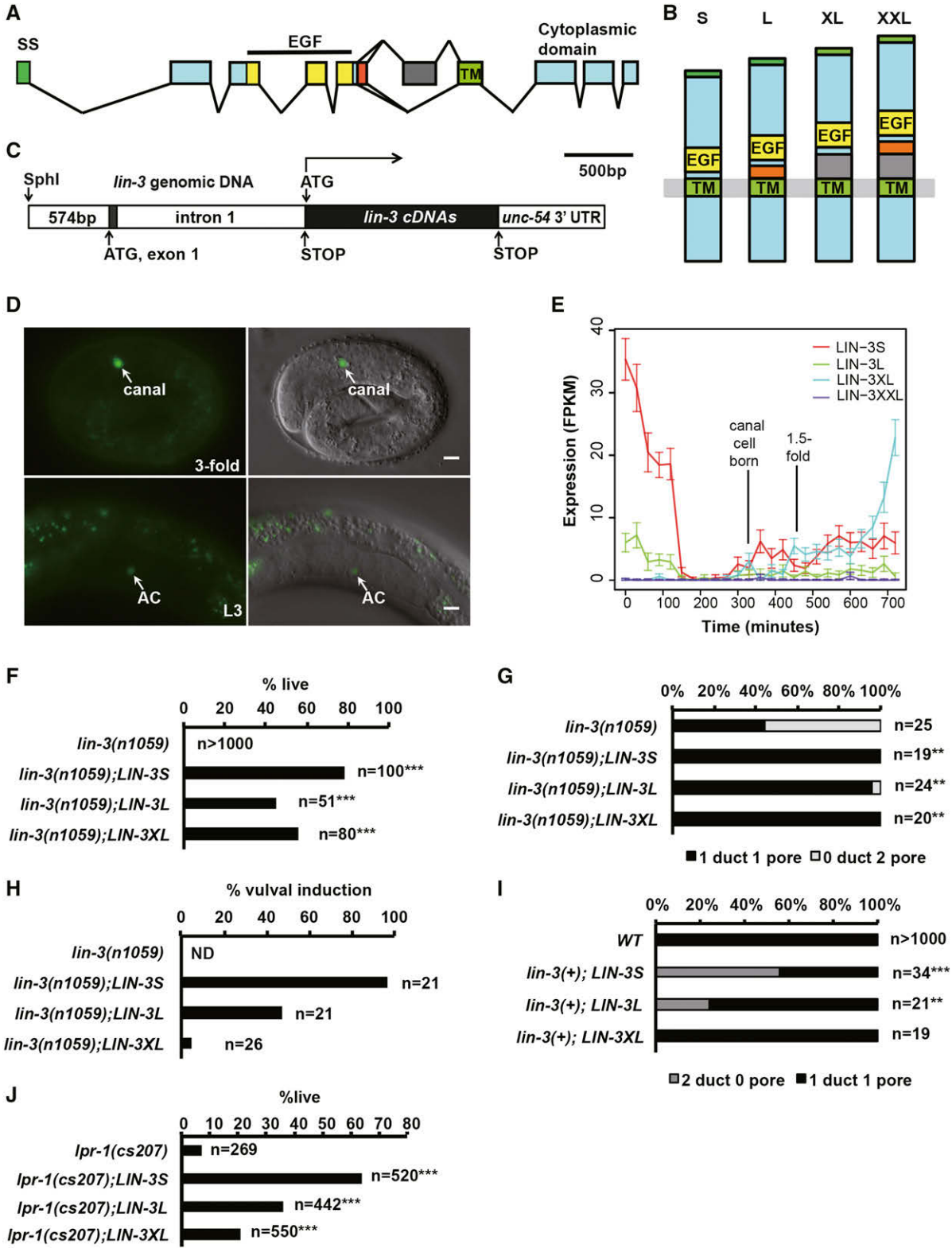

Figure 4 The predominant LIN-3/EGF isoform expressed in the excretory system signals with low efficiency. (A) Schematic of *lin-3* alternative splicing, based on Van Buskirk and Sternberg (2007). Exons are represented by boxes, and introns by lines, with colors indicating encoded domains. Orange and gray regions encode extracellular domains specific to certain splice isoforms. EGF, EGF-like domain (yellow); SS, secretion signal (green); TM, transmembrane domain (light green). (B) Schematic structure of four LIN-3 protein isoforms, with domains colored as in (A). See File S3 for corresponding sequences. (C) Schematic of single-copy MosSCI transgenes expressing different LIN-3 isoforms under control of the *lin-3* proximal promoter. *lin-3* cDNAs were inserted downstream of the first *lin-3* intron and an artificial stop codon, at the position of the second potential start codon. See File S2 and *Materials and Methods* for details. (D) Expression pattern of *lin-3p*::NLS::GFP transcriptional reporter at threefold (arrows point to canal cell) and at L3

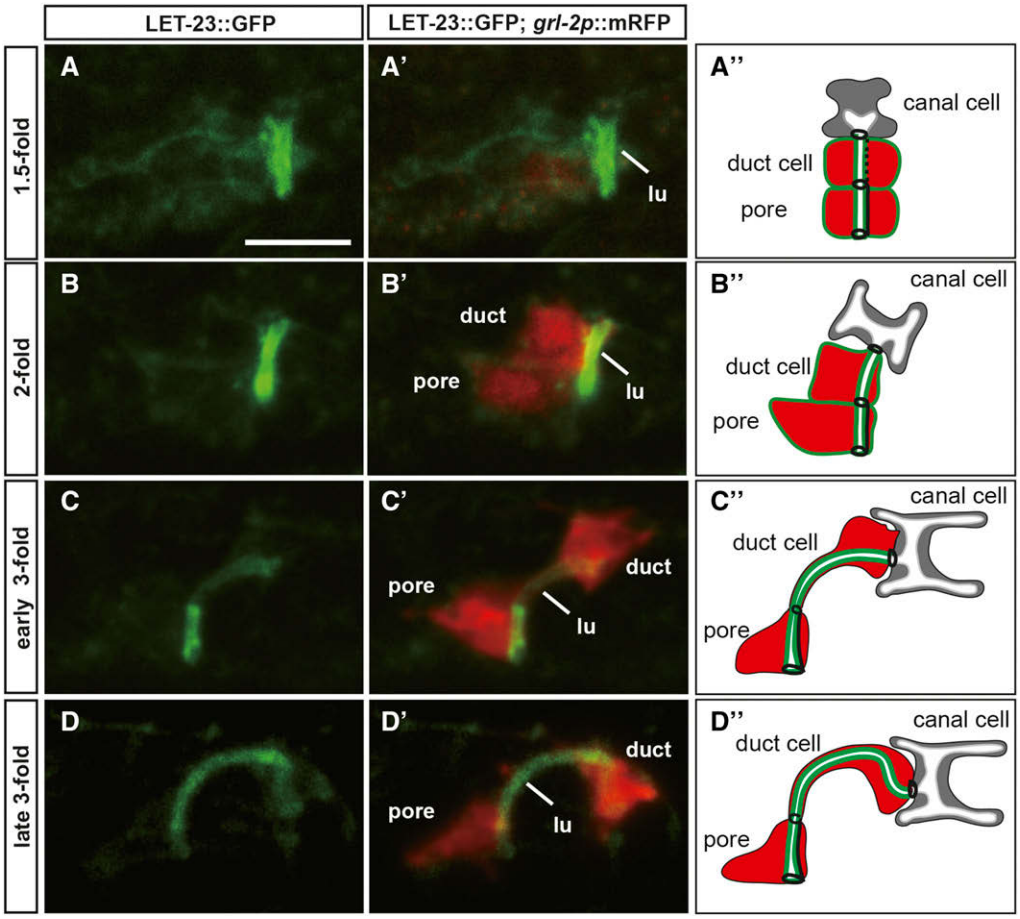

Figure 5 Apical localization of LET-23::GFP during duct and pore tube elongation. (A–D) LET-23::GFP (*zhIs038*; Haag *et al.* 2014) localization in the excretory system at different embryonic stages. (A′–D′) Corresponding overlays with duct and pore cell marker *grl-2p*::mRFP. (A″–D″) Schematic interpretations of results. LET-23::GFP was present initially at both apical and basolateral membrane domains of the duct and pore, but present exclusively at apical domains later in embryogenesis. Bar, 5 μM. lu, lumen.

Ras signaling is sufficient to bypass *lpr-1*, it does not appear to be required for lumen integrity either on its own or in parallel to *lpr-1*.

Discussion

Growth and elongation of unicellular tubes requires addition of new apical membrane and stabilization of the relatively narrow apical/luminal compartment. We showed that the secreted lipocalin LPR-1 is required to maintain apical membrane integrity and a continuous lumen in the *C. elegans* excretory duct and pore tubes during a period of lumen elongation. EGF-Ras-ERK signaling promotes the more elongated duct tube fate, and increased signaling within the duct and pore just prior to fate determination can bypass the requirement for LPR-1. Below we discuss possible models for the relationship between LPR-1 and EGF-Ras-ERK signaling and their roles in lumen growth and stabilization.

Relationship between LPR-1 and EGF-Ras-ERK signaling

Two general genetic models can explain bypass suppression such as that observed for *lpr-1* null mutants by increased LIN-3/EGF signaling. A simple linear pathway model would postulate that LPR-1 facilitates EGF signaling, such that the primary defect in *lpr-1* mutants is inadequate signaling (Figure 6A). An alternative parallel pathway model would postulate that LPR-1 and EGF signaling provide separate inputs into a common downstream process important for lumen integrity (Figure 6B).

Several observations appear inconsistent with a linear model in which LPR-1 facilitates LIN-3/EGF signaling from the canal cell to the duct and pore. First, *lpr-1* mutations did not perturb EGF-dependent duct fate specification, and despite the fact that *lpr-1* is widely expressed in other epithelia, including the vulva, we did not detect any other phenotypes indicative of a general defect in EGF-Ras-ERK signaling (data not shown). Second, we could not find conditions where

[arrows point to anchor cell (AC)]. Left panels: fluorescent images of *lin-3p*::NLS::GFP. Right panels: overlay of DIC and fluorescent images. Bar, 5 μM. (E) Quantification of different *lin-3* mRNA expression levels from MODCODE (Gerstein *et al.* 2010). (F–J) Functional studies of LIN-3 isoforms using single-copy MosSCI transgenes. (F–H) Rescue assays in the *lin-3(n1059)* null background. (I and J) Assays in a *lin-3(+)* background. In (G) and (I), duct *vs.* pore cell fates were assessed by AJM-1::GFP; *lin-3(n1059)* single mutant data are reproduced from Abdus-Saboor *et al.* (2011). Note that LIN-3S and LIN-3L did not cause a two duct phenotype in the *lin-3(n1059)* background, consistent with physiological levels of expression. In all graphs, $^{**}P < 0.01$ and $^{***}P < 0.0001$ compared to nontransgenic control (Fisher's exact test).

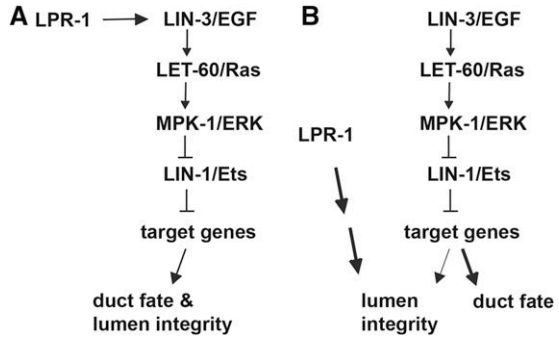

Figure 6 Two possible models for the relationship between LPR-1 and EGF-Ras-ERK-signaling pathway. (A) LPR-1 functions upstream of LIN-3/EGF. (B) LPR-1 functions in parallel to LIN-3/EGF. The data support the latter model. See text for details.

reduced signaling could phenocopy *lpr-1* mutants, suggesting that signaling is not required for lumen integrity. Furthermore, *lpr-1* mutation did not abolish activity of any specific LIN-3/EGF isoform or detectably affect LET-23/EGFR localization. We were unable to detect phosphorylated MPK-1/ERK in WT embryos (data not shown), so we could not directly test whether *lpr-1* affected pathway activation. Although we cannot completely exclude the possibility that LPR-1 facilitates LIN-3/EGF signaling through some other mechanism, we favor the model that LPR-1 and EGF-Ras-ERK act in parallel. Since reduced signaling did not enhance *lpr-1* null mutant defects, this parallel model implies that signaling normally plays only a minor role in lumen integrity, yet when increased is sufficient to bypass the LPR-1 requirement.

Given that loss of LIN-1/Ets, a known MPK-1/ERK substrate (Jacobs *et al.* 1998), efficiently suppresses *lpr-1*, a reasonable model is that increased signaling antagonizes LIN-1 to transcriptionally upregulate some target(s) that can compensate for *lpr-1* absence (Figure 6B). What could these targets be? Our data do not support one obvious possibility, which is that signaling upregulates other compensating lipocalins, since we found no evidence that related lipocalins could substitute for LPR-1. Instead, we favor models where both LPR-1 and EGF signaling affect membrane lipids and/or the apical extracellular matrix (aECM), which are needed for lumen growth and maintenance. Notably, the *lpr-1* mutant phenotype strongly resembles that caused by loss of the early aECM component LET-653 (Gill *et al.* 2016). However, *lpr-1* loss did not disrupt LET-653 secretion or localization in the duct (Gill *et al.* 2016). Furthermore, LET-653 OE could not suppress *lpr-1* mutant defects (Figure S3), arguing against the model that *let-653* is the key target upregulated by Ras signaling.

Lipocalins are best known as sterol, lipid, and fatty acid binding proteins (Flower 1996), and can interact with specific receptors to deliver lipophilic cargoes to target cells (Flower 2000). One possibility is that LPR-1 delivers some such cargo to the excretory duct and pore, although our data indicate that LPR-1 can function even when undetectable (by fluorescence) in those cells. Ras signaling can have widespread effects on cellular metabolism and lipid catabolism (Kamphorst *et al.* 2013; Kerr *et al.* 2016); therefore, Ras signaling may compensate for loss of LPR-1 by providing an alternative source of the missing metabolite. Further tests of these models will require biochemical identification of the LPR-1 cargo. We have also identified other suppressors of the *lpr-1* mutant phenotype, whose molecular characterization may provide additional insights.

Varied activities of different LIN-3/EGF isoforms

The excretory canal cell is one major source, though probably not the only relevant source, of LIN-3/EGF expression during excretory duct development (Abdus-Saboor *et al.* 2011). Our RNA-seq analysis suggests that multiple *lin-3* isoforms are expressed in the embryonic canal lineage, and each is capable of rescuing the excretory duct fate in *lin-3* null mutants. However, the predominant isoform, *lin-3(XL)*, is much less potent at converting the excretory pore cell into a second duct cell, suggesting it cannot function efficiently at a distance.

EGF family ligands are initially produced as transmembrane precursors, but proteolysis by ADAM-17 or Rhomboid-family proteases typically occurs in the juxtamembrane region to release the active EGF peptide for paracrine signaling (Sahin *et al.* 2004; Adrain and Freeman 2014). The different splice isoforms of *C. elegans* LIN-3/EGF differ in the region that would be expected to confer protease specificity, so the different biological activities observed for these isoforms might reflect different availabilities of isoform-specific proteases. Prior studies have suggested that LIN-3(L) activity uniquely depends on the Rhomboid-related protease ROM-1 (Dutt *et al.* 2004), but proteases acting on LIN-3(XL) or the other LIN-3/EGF isoforms are not known. It is possible that some isoforms of LIN-3/EGF remain uncleaved and thereby signal only in a juxtacrine manner (Singh and Harris 2005). Since the excretory canal cell directly contacts the excretory duct around the time of cell fate specification (Abdus-Saboor *et al.* 2011), it could be advantageous for this signaling event to use a juxtracrine mechanism. Unfortunately, our attempts to visualize LIN-3 have not yet been successful, so the location of LIN-3(XL) and whether or not it is cleaved remains unknown.

Localization and function of LET-23/EGFR in the excretory duct and pore

ErbB family receptors have been observed to localize to either basolateral or apical surfaces of epithelial cells, depending on the cell type and developmental stage (Wiley *et al.* 1992; Nouwen and De Broe 1994; Gesualdo *et al.* 1996; Nakagawa *et al.* 1997; MacRae Dell *et al.* 2004). For example, during *C. elegans* vulval development, LET-23/EGFR is initially enriched at basolateral surfaces of the vulval precursor cells, adjacent to the anchor cell, which is the relevant source of LIN-3/EGF (Kaech *et al.* 1998). This basolateral localization is important for efficient signaling. However, after signaling initiates, LET-23 partly relocates to apical surfaces, where it

may be sequestered from further interactions with LIN-3 (Haag *et al.* 2014). In the excretory system, we found that LET-23 localized to both basolateral and apical surfaces of the duct and pore during early tubulogenesis, but then relocated exclusively to the apical surfaces at later stages. This change could potentially sequester LET-23 from further interactions with LIN-3, if LIN-3 is basally secreted from the canal cell. Alternatively, it could facilitate continued signaling if LIN-3 is apically secreted from the canal cell or retained at the canal-duct junction in a transmembrane form. However, we found no evidence that continued signaling during embryonic development is essential for duct tube elongation, so any role of signaling during this period may be redundant with other mechanisms. Somewhat later, in the L1 stage, EGFR signaling through Ras is required in the duct to facilitate delamination of the excretory pore cell (Parry and Sundaram 2014). It will be interesting to determine if this is a case of luminal or juxtacrine signaling, and whether the LIN-3(XL) isoform is specialized for such signaling.

Acknowledgments

We thank Kevin Bickard and Claudia Lanauze for participation in the genetic screen that identified our new *lpr-1* alleles; Brian Gantick for assistance in generating some data; and Jennifer Cohen, Fabien Soulavie, and Rachael Forman-Rubinsky for helpful discussions and comments on the manuscript. We thank Cheryl Van Buskirk, Paul Sternberg, Alex Hajnal, and Todd Lamitina for sharing reagents, and Neil Hopper for providing the unpublished allele *sos-1(pd10gf)*. Some strains were obtained from the *Caenorhabditis* Genetics Center, which is funded by National Institutes of Health Office of Research Infrastructure Programs (P40 OD-010440). This work was supported by National Science Foundation grant #1257879 and American Heart Association grant #0755524U to M.V.S.

Literature Cited

Abdus-Saboor, I., V. P. Mancuso, J. I. Murray, K. Palozola, C. Norris *et al.*, 2011 Notch and Ras promote sequential steps of excretory tube development in C. elegans. Development 138: 3545–3555.

Adrain, C., and M. Freeman, 2014 Regulation of receptor tyrosine kinase ligand processing. Cold Spring Harb. Perspect. Biol. 6: a008995.

Aronson, D. E., L. M. Costantini, and E. L. Snapp, 2011 Superfolder GFP is fluorescent in oxidizing environments when targeted via the Sec translocon. Traffic 12: 543–548.

Bacaj, T., and S. Shaham, 2007 Temporal control of cell-specific transgene expression in Caenorhabditis elegans. Genetics 176: 2651–2655.

Brenner, S., 1974 The genetics of Caenorhabditis elegans. Genetics 77: 71–94.

Burdick, J., T. Walton, E. Preston, A. Zacharias, A. Raj, and J. I. Murray, 2016 Overlapping cell population expression profiling and regulatory inference in *C. elegans*. BMC Genomics 17: 159.

Chang, C., N. A. Hopper, and P. W. Sternberg, 2000 Caenorhabditis elegans SOS-1 is necessary for multiple RAS-mediated developmental signals. EMBO J. 19: 3283–3294.

Chou, C. M., C. Nelson, S. A. Tarle, J. T. Pribila, T. Bardakjian *et al.*, 2015 Biochemical basis for dominant inheritance, variable penetrance, and maternal effects in RBP4 congenital eye disease. Cell 161: 634–646.

Christoffersen, C., H. Obinata, S. B. Kumaraswamy, S. Galvani, J. Ahnstrom *et al.*, 2011 Endothelium-protective sphingosine-1-phosphate provided by HDL-associated apolipoprotein M. Proc. Natl. Acad. Sci. USA 108: 9613–9618.

Cui, M., J. Chen, T. R. Myers, B. J. Hwang, P. W. Sternberg *et al.*, 2006 SynMuv genes redundantly inhibit lin-3/EGF expression to prevent inappropriate vulval induction in C. elegans. Dev. Cell 10: 667–672.

Dittrich, A. M., H. A. Meyer, and E. Hamelmann, 2013 The role of lipocalins in airway disease. Clin. Exp. Allergy 43: 503–511.

Dutt, A., S. Canevascini, E. Froehli-Hoier, and A. Hajnal, 2004 EGF signal propagation during C. elegans vulval development mediated by ROM-1 rhomboid. PLoS Biol. 2: e334.

El Karoui, K., A. Viau, O. Dellis, A. Bagattin, C. Nguyen *et al.*, 2016 Endoplasmic reticulum stress drives proteinuria-induced kidney lesions via Lipocalin 2. Nat. Commun. 7: 10330.

Enriquez-de-Salamanca, A., S. Bonini, and M. Calonge, 2012 Molecular and cellular biomarkers in dry eye disease and ocular allergy. Curr. Opin. Allergy Clin. Immunol. 12: 523–533.

Fares, H., and I. Greenwald, 2001 Genetic analysis of endocytosis in Caenorhabditis elegans: coelomocyte uptake defective mutants. Genetics 159: 133–145.

Flo, T. H., K. D. Smith, S. Sato, D. J. Rodriguez, M. A. Holmes *et al.*, 2004 Lipocalin 2 mediates an innate immune response to bacterial infection by sequestrating iron. Nature 432: 917–921.

Flower, D. R., 1996 The lipocalin protein family: structure and function. Biochem. J. 318(Pt. 1): 1–14.

Flower, D. R., 2000 Beyond the superfamily: the lipocalin receptors. Biochim. Biophys. Acta 1482: 327–336.

Frokjaer-Jensen, C., M. W. Davis, C. E. Hopkins, B. J. Newman, J. M. Thummel *et al.*, 2008 Single-copy insertion of transgenes in Caenorhabditis elegans. Nat. Genet. 40: 1375–1383.

Gerstein, M. B., Z. J. Lu, E. L. Van Nostrand, C. Cheng, B. I. Arshinoff *et al.*, 2010 Integrative analysis of the Caenorhabditis elegans genome by the modENCODE project. Science 330: 1775–1787.

Gesualdo, L., S. Di Paolo, A. Calabro, S. Milani, E. Maiorano *et al.*, 1996 Expression of epidermal growth factor and its receptor in normal and diseased human kidney: an immunohistochemical and in situ hybridization study. Kidney Int. 49: 656–665.

Gill, H. K., J. D. Cohen, J. Ayala-Figueroa, R. Forman-Rubinsky, C. Poggioli *et al.*, 2016 Integrity of narrow epithelial tubes in the C. elegans excretory system requires a transient luminal matrix. PLoS Genet. 12: e1006205.

Gilleard, J. S., J. D. Barry, and I. L. Johnstone, 1997 cis regulatory requirements for hypodermal cell-specific expression of the Caenorhabditis elegans cuticle collagen gene dpy-7. Mol. Cell. Biol. 17: 2301–2311.

Glasgow, B. J., A. R. Abduragimov, Z. T. Farahbakhsh, K. F. Faull, and W. L. Hubbell, 1995 Tear lipocalins bind a broad array of lipid ligands. Curr. Eye Res. 14: 363–372.

Gouveia, S. M., and J. M. Tiffany, 2005 Human tear viscosity: an interactive role for proteins and lipids. Biochim. Biophys. Acta 1753: 155–163.

Gupta, B. P., W. Hanna-Rose, and P. W. Sternberg, 2012 Morphogenesis of the vulva and the vulval-uterine connection (30 November 2012), *Wormbook*, ed. The *C. elegans* Research Community WormBook, doi/ 10.1895/wormbook.1.152.1, http://www.wormbook.org.

Gwira, J. A., F. Wei, S. Ishibe, J. M. Ueland, J. Barasch *et al.*, 2005 Expression of neutrophil gelatinase-associated lipocalin regulates epithelial morphogenesis in vitro. J. Biol. Chem. 280: 7875–7882.

Haag, A., P. Gutierrez, A. Buhler, M. Walser, Q. Yang *et al.*, 2014 An in vivo EGF receptor localization screen in C. elegans identifies the Ezrin homolog ERM-1 as a temporal regulator of signaling. PLoS Genet. 10: e1004341.

Han, M., R. V. Aroian, and P. W. Sternberg, 1990 The let-60 locus controls the switch between vulval and nonvulval cell fates in Caenorhabditis elegans. Genetics 126: 899–913.

Hao, L., R. Johnsen, G. Lauter, D. Baillie, and T. R. Burglin, 2006 Comprehensive analysis of gene expression patterns of hedgehog-related genes. BMC Genomics 7: 280.

Hill, R. J., and P. W. Sternberg, 1992 The gene lin-3 encodes an inductive signal for vulval development in C. elegans. Nature 358: 470–476.

Hill, A. J., R. Mansfield, J. M. Lopez, D. M. Raizen, and C. Van Buskirk, 2014 Cellular stress induces a protective sleep-like state in C. elegans. Curr. Biol. 24: 2399–2405.

Jacobs, D., G. J. Beitel, S. G. Clark, H. R. Horvitz, and K. Kornfeld, 1998 Gain-of-function mutations in the Caenorhabditis elegans lin-1 ETS gene identify a C-terminal regulatory domain phosphorylated by ERK MAP kinase. Genetics 149: 1809–1822.

Joshi, S., and A. Viljoen, 2015 Renal biomarkers for the prediction of cardiovascular disease. Curr. Opin. Cardiol. 30: 454–460.

Kaech, S. M., C. W. Whitfield, and S. K. Kim, 1998 The LIN-2/LIN-7/LIN-10 complex mediates basolateral membrane localization of the C. elegans EGF receptor LET-23 in vulval epithelial cells. Cell 94: 761–771.

Kamphorst, J. J., J. R. Cross, J. Fan, E. de Stanchina, R. Mathew *et al.*, 2013 Hypoxic and Ras-transformed cells support growth by scavenging unsaturated fatty acids from lysophospholipids. Proc. Natl. Acad. Sci. USA 110: 8882–8887.

Kashani, K., and J. A. Kellum, 2015 Novel biomarkers indicating repair or progression after acute kidney injury. Curr. Opin. Nephrol. Hypertens. 24: 21–27.

Katz, W. S., R. J. Hill, T. R. Clandinin, and P. W. Sternberg, 1995 Different levels of the C. elegans growth factor LIN-3 promote distinct vulval precursor fates. Cell 82: 297–307.

Kerr, E. M., E. Gaude, F. K. Turrell, C. Frezza, and C. P. Martins, 2016 Mutant Kras copy number defines metabolic reprogramming and therapeutic susceptibilities. Nature 531: 110–113.

Koppen, M., J. S. Simske, P. A. Sims, B. L. Firestein, D. H. Hall *et al.*, 2001 Cooperative regulation of AJM-1 controls junctional integrity in Caenorhabditis elegans epithelia. Nat. Cell Biol. 3: 983–991.

MacRae Dell, K., R. Nemo, W. E. Sweeney, Jr., and E. D. Avner, 2004 EGF-related growth factors in the pathogenesis of murine ARPKD. Kidney Int. 65: 2018–2029.

Mulligan, K. A., C. Fuerer, W. Ching, M. Fish, K. Willert *et al.*, 2012 Secreted Wingless-interacting molecule (Swim) promotes long-range signaling by maintaining Wingless solubility. Proc. Natl. Acad. Sci. USA 109: 370–377.

Nakagawa, T., Y. Hayase, M. Sasahara, M. Haneda, R. Kikkawa *et al.*, 1997 Distribution of heparin-binding EGF-like growth factor protein and mRNA in the normal rat kidneys. Kidney Int. 51: 1774–1779.

Nouwen, E. J., and M. E. De Broe, 1994 EGF and TGF-alpha in the human kidney: identification of octopal cells in the collecting duct. Kidney Int. 45: 1510–1521.

Parry, J. M., and M. V. Sundaram, 2014 A non-cell-autonomous role for Ras signaling in C. elegans neuroblast delamination. Development 141: 4279–4284.

Quadro, L., W. S. Blaner, D. J. Salchow, S. Vogel, R. Piantedosi *et al.*, 1999 Impaired retinal function and vitamin A availability in mice lacking retinol-binding protein. EMBO J. 18: 4633–4644.

Robinson, J. T., H. Thorvaldsdottir, W. Winckler, M. Guttman, E. S. Lander *et al.*, 2011 Integrative genomics viewer. Nat. Biotechnol. 29: 24–26.

Rocheleau, C. E., R. M. Howard, A. P. Goldman, M. L. Volk, L. J. Girard *et al.*, 2002 A lin-45 raf enhancer screen identifies eor-1, eor-2 and unusual alleles of Ras pathway genes in Caenorhabditis elegans. Genetics 161: 121–131.

Rose-John, S., 2013 ADAM17, shedding, TACE as therapeutic targets. Pharmacol. Res. 71: 19–22.

Saffer, A. M., D. H. Kim, A. van Oudenaarden, and H. R. Horvitz, 2011 The Caenorhabditis elegans synthetic multivulva genes prevent ras pathway activation by tightly repressing global ectopic expression of lin-3 EGF. PLoS Genet. 7: e1002418.

Sahin, U., G. Weskamp, K. Kelly, H. M. Zhou, S. Higashiyama *et al.*, 2004 Distinct roles for ADAM10 and ADAM17 in ectodomain shedding of six EGFR ligands. J. Cell Biol. 164: 769–779.

Saxena, A., B. Denholm, S. Bunt, M. Bischoff, K. VijayRaghavan *et al.*, 2014 Epidermal growth factor signalling controls myosin II planar polarity to orchestrate convergent extension movements during Drosophila tubulogenesis. PLoS Biol. 12: e1002013.

Schindelin, J., I. Arganda-Carreras, E. Frise, V. Kaynig, M. Longair *et al.*, 2012 Fiji: an open-source platform for biological-image analysis. Nat. Methods 9: 676–682.

Schneider, C. A., W. S. Rasband, and K. W. Eliceiri, 2012 NIH Image to ImageJ: 25 years of image analysis. Nat. Methods 9: 671–675.

Singh, A. B., and R. C. Harris, 2005 Autocrine, paracrine and juxtacrine signaling by EGFR ligands. Cell. Signal. 17: 1183–1193.

Sternberg, P. W., and H. R. Horvitz, 1986 Pattern formation during vulval development in C. elegans. Cell 44: 761–772.

Stone, C. E., D. H. Hall, and M. V. Sundaram, 2009 Lipocalin signaling controls unicellular tube development in the Caenorhabditis elegans excretory system. Dev. Biol. 329: 201–211.

Trapnell, C., L. Pachter, and S. L. Salzberg, 2009 TopHat: discovering splice junctions with RNA-Seq. Bioinformatics 25: 1105–1111.

Trapnell, C., B. A. Williams, G. Pertea, A. Mortazavi, G. Kwan *et al.*, 2010 Transcript assembly and quantification by RNA-Seq reveals unannotated transcripts and isoform switching during cell differentiation. Nat. Biotechnol. 28: 511–515.

Van Buskirk, C., and P. W. Sternberg, 2007 Epidermal growth factor signaling induces behavioral quiescence in Caenorhabditis elegans. Nat. Neurosci. 10: 1300–1307.

Wang, X., H. Jia, and H. M. Chamberlin, 2006 The bZip proteins CES-2 and ATF-2 alter the timing of transcription for a cell-specific target gene in C. elegans. Dev. Biol. 289: 456–465.

Wiley, L. M., J. X. Wu, I. Harari, and E. D. Adamson, 1992 Epidermal growth factor receptor mRNA and protein increase after the four-cell preimplantation stage in murine development. Dev. Biol. 149: 247–260.

Wu, Y., and M. Han, 1994 Suppression of activated Let-60 ras protein defines a role of Caenorhabditis elegans Sur-1 MAP kinase in vulval differentiation. Genes Dev. 8: 147–159.

Zhang, Z., E. Pascuet, P. A. Hueber, L. Chu, D. G. Bichet *et al.*, 2010 Targeted inactivation of EGF receptor inhibits renal collecting duct development and function. J. Am. Soc. Nephrol. 21: 573–578.

Communicating editor: P. Sengupta